World Applied Sciences Journal 15 (11): 1494-1502, 2011
ISSN 1818-4952

Obtaining Optimal Performance with Ring Stiffeners on Strength for Submarine Pipeline

[1]Farhad Riahi, [2]Abolfazl Shamsai, [1]Kamal Rahmani and [3]Hossein Showkati

[1]Department of Civil Engineering, Mahabad Branch, Islamic Azad University, Mahabad, Iran
[2]Department of Civil Engineering, Sharif University of Technology, Tehran, Iran
[3]Department of Civil Engineering, Urmia University, Urmia, Iran

Abstract: Submarine pipelines as the principal structural components are prone to fail by circumferential buckling under the effect of hydrostatic external pressure. Basically, the buckling capacity of a thin-walled pipe is dependent on "radius to thickness" ratio. At least two modes of local and overall buckling are possible in any pipeline system, which could be developed in pipe wall. A method of strengthening of pipes is developed in this paper to stop the failure. A total of 21 stiffened models are generated and analyzed using the well-known finite element program ABAQUS. In this study, the buckling and post-buckling behaviour of stiffened pipes are investigated by carrying out linear and nonlinear analyses. The nonlinear finite element analysis presented in this paper is a parametric study which focuses on evaluating results sensitivity to ABAQUS nonlinear solution method of modified Riks arc-length solution algorithm. The results of inelastic Riks ultimate strength analysis cover a wide range of typical geometric ratios. For a precise post-buckling analysis, material and geometrical nonlinear analysis are considered. Once a nonlinear finite element study is conducted, comparison was made on the load-displacement response, ultimate strength and failure modes of pipelines. It was concluded that the proposed stiffening method is quite economical.

Key words: Submarine Pipelines · Stiffening · Buckling · Ring tilting · Hydrostatic pressure

INTRODUCTION

Submarine pipeline is a convenient means to transport crude oil or natural gas from offshore oil wells to an onshore location [1]. Recent advances in pipe manufacturing techniques and pipeline construction have enabled the installation of larger diameter pipeline in ultra- deepwater locations [2]. Pipelines employed in deep water offshore activities are responsible for substantial amount of the total costs of a field development.

In case of steel pipes the reduction of costs is directly related to the thickness optimization. Furthermore, pipeline buckling caused to collapse much long pipeline with a loss of several millions of dollars for the oil companies, environmental protections, etc, [3]. Therefore, this is important to design and manufacture economically the pipeline.

A major type of compression element used in submarine pipelines is the fabricated steel cylindrical shell, which is stiffened against buckling by ring and/or stringer stiffeners. An extensive number of theoretical and experimental studies have been performed on buckling of cylindrical shells over past years. The increasing offshore application of stiffened submarine pipelines, especially in deep water, has raised new questions still needed to be resolved. Ring stiffeners to strengthen submarine pipelines are very effective against loading by external pressure.

On the other hand, rings or ring beams are often used to stiffen pressurized vessels [4] and deep water pipelines. These rings cause to increase the buckling strength of pipeline and also increase the operation of pipeline consequently reduce the pipeline's thickness which was previously explained. The buckle propagation in circular cylindrical shells under hydrostatic pressure is a post buckling phenomenon causing a progressive structural failure.

The buckle propagation of pipelines was initially considered by Johns *et al*. [5], but the first paper on the subject with a proposed equation for the propagation pressure was originated from an independent investigation by palmer [6] based on the strain energy of the collapsed cross section the results underestimated the experimental values for low ratios between external diameter and thickness (D/t) [7, 8].

Corresponding Author: Kamal Rahmani, Department of Civil Engineering,
Mahabad Branch, Islamic Azad University, Mahabad, Iran.

The first experimental studies were performed by Johns *et al*. [5] who tested different arrestors geometries used to stop the buckle propagation. based on his studies an empirical formula was proposed [5, 6] to evaluate the propagation pressure (Pp) as a function of both D/t ratio and material yield strength (σ_0):

$$\frac{Pp}{\sigma_0} = 6\left(\frac{2t}{D}\right)^{2.5} \quad (1)$$

A theoretical expression for the propagation pressure which is based on the internal energy dissipation of a simplified ring model was proposed by Pasqualino and Estefen [9].

The ring section was modeled with the aid of curved beam elements considering material strain hardening. Although they have presented good correlation with some experimental results, in general the proposed expression overestimated the propagation pressure [10, 11].

$$\frac{p_p}{\sigma_0} = \frac{4}{\pi}\left(\frac{2t}{D}\right)^2\left[1.0 + 2.07\left(\frac{2t}{D}\right)^{0.35}\left(\frac{E_t}{\sigma_0}\right)^{0.12}\right] \quad (2)$$

Kamalarasa and Calladine [12] extended Palmer approach to three- dimensional model. A good correlation with experimental results was achieved but the proposed method requires experimental tests for the prediction of the propagation pressure.

In this paper the critical buckling pressure and post-buckling pressure and propagating buckling pressure under hydrostatic pressure of water on small scale pipelines with rings were obtained.

Geometries and Properties of Test Specimens and Instruments

Geometries of the Models: In all, 21 tests were performed. In specimens (L/R) =50, (R/t) =200, have been employed. The geometric properties of rings were such r_{inner}/t_r =30.

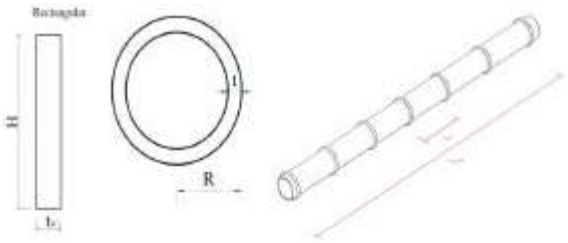

Fig. 1: Nominal geometrical pipe and Ring Stiffener's models

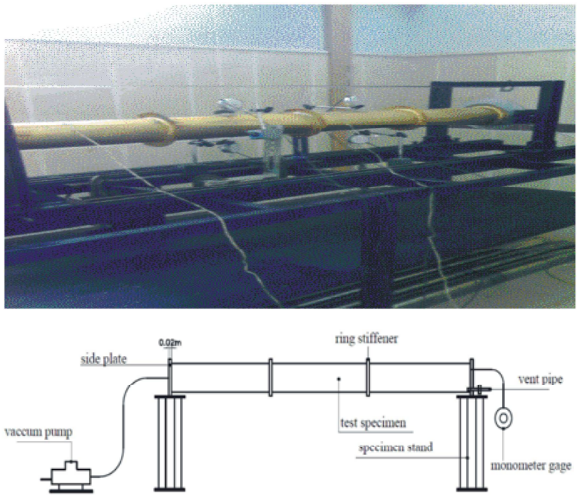

Fig. 2: Specimen and Test Overview

Specimens was labelled such that the parameters that were difference between specimens could be identified. For example ∴RR∴ indicated that this specimen ∴ have rings number with equal space between rings and other specimen ∴ have high stiffener and RR; section of ring is rectangular. Fig. 1 shows nominal geometrical pipe and Ring Stiffener's models.

Table 1 summarize the pipeline geometric parameters such as inner and outer diameters, wall thickness and length. Ring Stiffener's and the properties of specimens are shown in Table 2. Fig. 2 shows the picture of testing pipeline set up and schematic diagram of the experimental set up for the specimen and testing purposes. Table 3 Indicates the properties of the specimens.

Table 1: Pipe geometric parameters

Specimen	inner radius (mm)	Outer radius (mm)	L_0, length (mm)	Thickness (mm)
Pipe	59.97	60	3000	0.3

Table 2: Ring Stiffener's geometric parameters

Specimen	inner radius (mm)	Thickness (mm)	high stiffener (mm)
Ring Stiffener	60	2	5-10-15-20-25

Table 3: Indicate the properties of specimens

Specimen label	stiffener's height (mm)	Rings space, L (mm)	Rings number
P0	-	-	-
2RR5	5	1440	2
2RR10	10	1440	2
2RR15	15	1440	2
2RR20	20	1440	2
2RR25	25	1440	2
4RR5	5	960	4
4RR10	10	960	4
4RR15	15	960	4
4RR20	20	960	4
4RR25	25	960	4
7RR5	5	480	7
7RR10	10	480	7
7RR15	15	480	7
7RR20	20	480	7
7RR25	25	480	7
13RR5	5	240	13
13RR10	10	240	13
13RR15	15	240	13
13RR20	20	240	13
13RR25	25	240	13

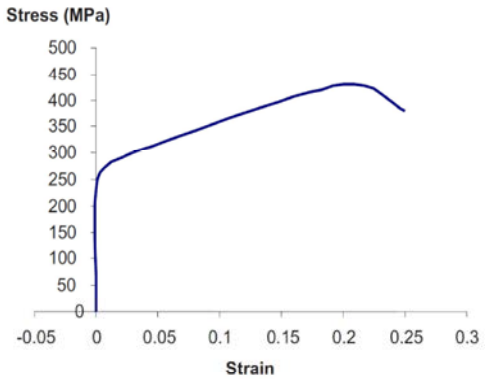

Fig. 3: Tensile stress strain relation of material

Properties of The Models: A load path represented by pressure followed to generate lower bound collapse loads. For each steel series one model has been submitted to the load by pressure just to approve that it generates higher collapse pressure compared with the opposite load path adopting. Although the steel Young's modulus is respective stress–strain curves in the plastic regime presented [13, 16, 17]. The pipeline is considered to be made of steel. The stress–strain relationship of such material can be described as linear elastic power law hardening. ε_{yp}= 0.002 the yield strain, υ =0.3 the Poisson's ratio and E =211 Gpa the Young's modulus. Under the action of external pressure, the uniform ring undergoes elastic–plastic collapse. Fig. 3 depicts the tensile stress which is related to pipeline material.

Buckling Analysis by Finite Element Method (FEM): Finite element analysis Futures Education Association is the most common structural analysis tool in use today. Great strides have been made in theoretical and computational aspects of FEA. In offshore industries, the use of this technique is becoming more widespread in design, reliability and risk analysis and performance evaluation of offshore structures.

Buckling analysis is a technique used to determine buckling loads - critical loads at which a structure becomes unstable - and buckled mode shapes - the characteristic shape associated with a structure's buckled response. This Section summarizes the fundamental principles and technical background related to buckling analysis by finite element method (FEM). The detailed information can be found in ABAQUS Program Release 6.8.1 Documentation Preview for performing the buckling analysis [13].

A propagating buckle will cause the formation of a transition zone, which connects the un-buckled region with the buckled. Fig. 1 shows a transition zone in a buckle propagation uniform pipeline. The pre-and post-buckling behaviours of the pipeline with Integral buckle arrestors model Young's modulus E in an ABAQUS Standard program. The collapse modes of the pipeline with Integral buckle arrestors are generated from ABAQUS post-analysis. RIKS procedure is used to analyze the unstable collapse of the pipeline with Integral buckle arrestors. In each step of analysis, the external pressure is incremented using a load proportional factor and NLGEOM parameter is included to account for the geometric nonlinearity. Fig. 4 shows the buckle propagation in a pipeline.

Ultimate Strength under External Pressure: Unstiffened pipelines under external hydrostatic pressure are subjected to elastic or inelastic local buckling of the shell wall between restraints. Once initiated, the collapse will tend to flatten the member from one end to the other. Similarly, ring-stiffened members are subject to local buckling of the shell wall between rings. The shell buckles between the rings, while the rings remain essentially circular.

Theoretically, the resistance of a pipeline decreases after the bifurcation point is reached, so the buckling strength is equal to the ultimate strength of the pipeline,

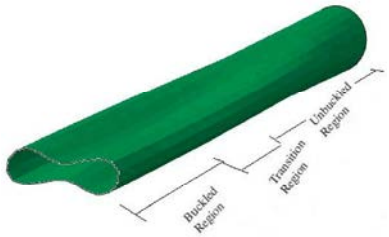

Fig. 4: Buckle propagation in a pipeline

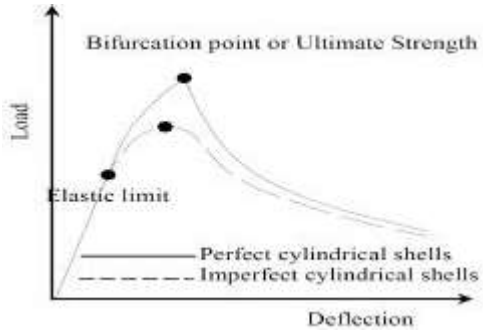

Fig. 5: Buckling and Post buckling Behavior of Cylindrical Shells

as shown in Figure 4. However, initial imperfections have a detrimental effect on load-carrying capacity due to the very unstable post buckling behaviour of pipeline. Therefore initial imperfections should be monitored carefully during fabrication, assembly and installation [18-20]. Buckling and Post buckling Behavior of Cylindrical Shells are shown in Fig. 5.

Analysis tests have been conducted for 21 series of pipe models Graphs indicate that curvature start to rising flexibility after loading and after rising the pressure to a significant magnitude specimen buckle and this is the local buckling because of that only the small part of shell buckled, this part of graph indicate the elastic buckling region of specimen. Therefore, the curvature enter to the post-buckling region of graph and we can see the most important part of the numerical means buckling propagating, the local buckling of specimen propagate along the space between two ring stiffener.

Buckling Initiation and Propagation: For a member with a non-compact section, the local buckling may occur before the member as a whole becomes unstable or before the yield point of the material is reached. Such behavior is characterized by local distortions of the cross section of the member. When a detailed analysis is not available, the equations given as below may be used to evaluate the local buckling stress for the member with a non-compact section.

Once the local buckle has occurred, the buckle will propagate along the pipeline until the external pressure becomes less than the buckle propagation pressure. In other words, the buckle propagation may occur if the external pressure exceeds the propagation pressure for the pipeline. Buckle propagation can be prevented by increasing the wall thickness to the buckle propagation thickness or by designing ring stiffeners spaced along the pipeline. The space between two ring stiffeners is defined based on cost and risk optimization. The external surfaces have been mapped before and after the damage simulations in order to use the data as input to especially implemented software for the definition of the respective actual geometrical imperfection distributions. Parameter f_0 indicated below is used to define cross-sectional damage magnitude as function of maximum and minimum local diameters.

$$f_0 = \frac{(D_{MAX} - D_{MIN})}{(D_{MAX} + D_{MIN})} \quad (3)$$

Each model was put inside and submitted to quasi-static external pressure loading up to first collapse (initiation pressure), which was characterized by a sudden loud noise and a simultaneous drop of pressure. Pipelines can buckle due to the hydrostatic pressure, in other words due to the pressure that applies on the outer surface of the pipe, P_e. This buckling state is known as collapse. This phenomenon can occur in deepwater, where the pressure differential Pr between the external and the internal pressures overtakes a limit pressure called critical pressure Pc. This pressure Pc is a function of the pipe dimensions.

The following equations based on the work of Timoshenko and Haagsma are widely used for the calculation of the critical pressure Pc. The expression is defined in the British Standards as well as in DNV codes [7, 8, 10].

$$(P_c - P_{el}).(P_{c_2} - P_{p_2}) = P_c.P_{el}.P_p.f_0.\left(\frac{D_0}{t}\right) \quad (4)$$

Where D_0 is the nominal pipe diameter; t is the pipe wall thickness and the pipe mechanical characteristics is define as:

E is Young's modulus of the pipe material; υ is Poisson's coefficient of the pipe material; σ_y is yield stress of the pipe wall material.

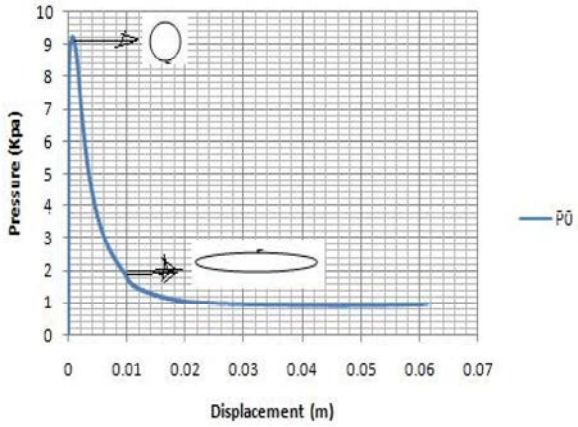

Fig. 6: Graph indicate these variations

Fig. 7: Shape is indicated these variations

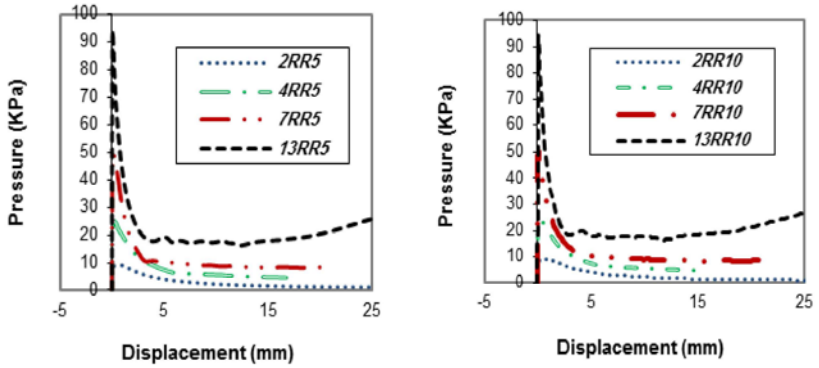

Fig. 8: Pressure- Displacement of specimens by 5 and 10 mm high stiffener

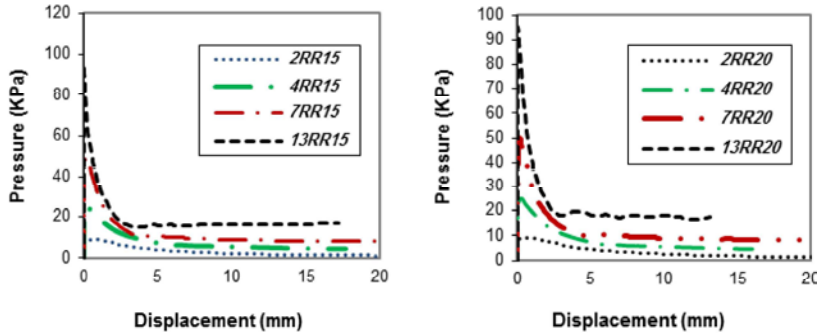

Fig. 9: Pressure- Displacement of specimens by 15 and 20 mm high stiffener

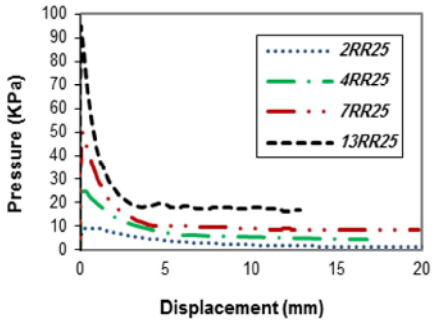

Fig. 10: Pressure- Displacement of specimens by 25 mm high stiffener

Following the local buckling state, pipelines may be subjected to propagation buckling [10-12]. It is important to understand that this state of failure cannot occur unless a local buckle has previously occurred. Depending on the type of pipeline submarine, the propagation buckle will be driven by different factors.

In the case of submarine pipelines, the hydrostatic pressure, or external pressure is responsible for the propagation buckling.

In both cases, a local buckle will propagate along the pipeline if the external pressure exceeds a critical value known as the propagation pressure P_{pr}.

The determination of this critical pressure is essential for the design of deep-water pipelines. Buckling propagation phenomena is observed in post-buckling region as mentioned before local buckling create a small failure on shell of specimen such a circular shape then this shape develop to oval shape with rising pressure as well. This shape develop along the panel between two rings extremely with reaching the buckling propagation to rings and reaching specimen's pressure to failure pressure, oval shape become change to hexangular shape.

In each shape change one has to observe a variation in curvature's gradient for example a graph indicate these variations in Fig. 6. These shapes are also indicated in Fig. 7.

Diagram Ultimate Strength of the Pipe Models: In Figs. 8-10, the radial deformations of all specimens are plotted in some selected nodes of pipe wall. It is evident at the buckling stage that the defections grow rapidly. Moreover, it was concluded that the amount of radial defection considerably declines by decreasing the stiffeners 'distance. In addition, the failure modes of specimens are shown in Figs. 11- 14.

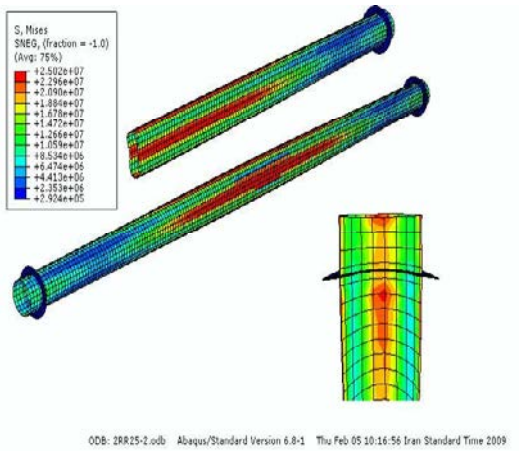

Fig. 11: Collapsed of the models and specimens 2 rings

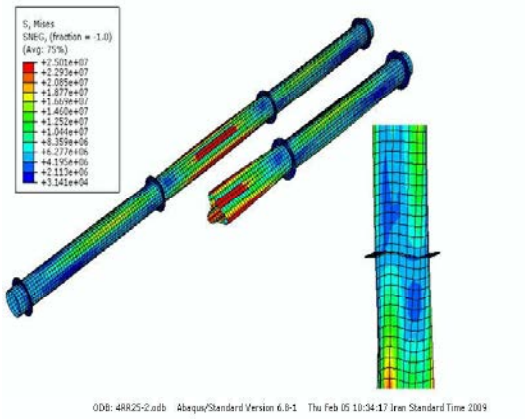

Fig. 12: Collapsed of the models and specimens 4 rings

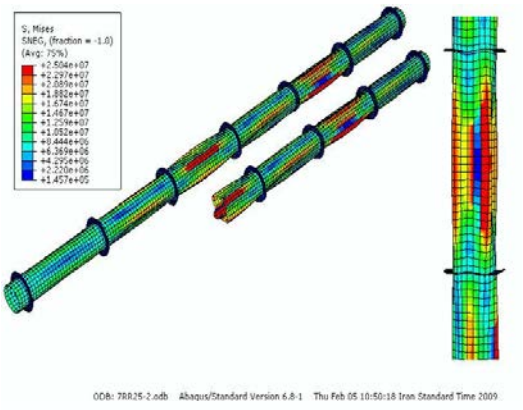

Fig. 13: Collapsed of the models and specimens 7 rings

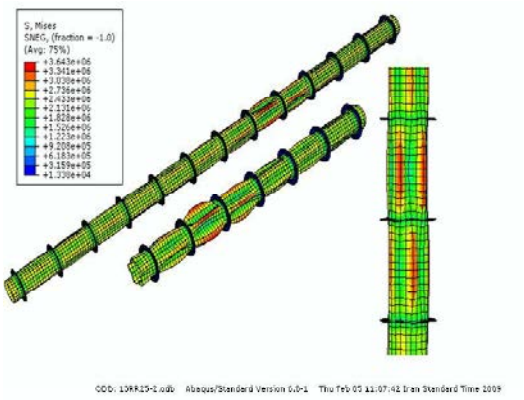

Fig. 14: Collapsed of the models and specimens 13 rings

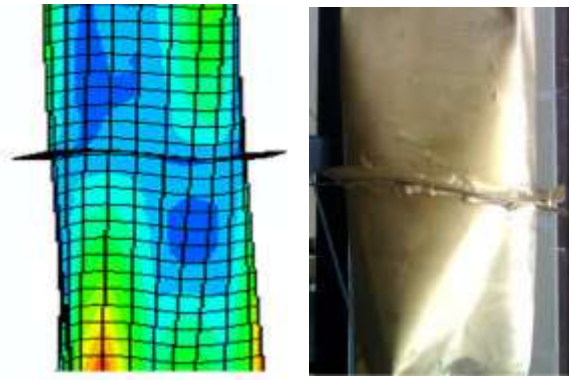

Fig. 15: Out-of-plane buckling of thin ring: FE specimen and test specimen

Verification of Rings Tilting: Along the tests, an out-of-plane deformation of ring stiffeners were experienced. Each ring provides an effective radial restraint against pipe buckling to some extent of pipe length. Therefore, all the rings are theoretically located at infection points of axial buckling mode. Rotation of pipe wall at the points causes the rings to tilt laterally, when they are manufactured from thin- walled slender sections.

This phenomenon is classified as a mode of lateral buckling which is strongly dependent to torsional properties of rings. The mode number of ring tilting in this case is consistent with the circumferential mode buckling of the pipe.

Fig. 15 shows a sample of such behaviour during experimental research program of the presentation of data in this paper.

Strength Assessment: Numerical results for the analysis tests on initiation buckling are indicated in the stated Table 4 for the specimen label.

The pipe á,â characteristics are the ratios pressure differential models by last model for example P2 ring, P0 and P4 ring; P2 ring and P7ring; P4ring and P13ring; P7ring are:

$$Z = \frac{\rho_{u_i} - \rho_{u(i-1)}}{\rho_{u(i-1)}} \times 100 \quad (5)$$

Table 4: Specimen label ∴RR∴

Specimen label	P_{cr}	P_u	ρ	Z	α	β	γ	n
P0	5.19	8.18	-	-	-	-	-	2
2 RR5	6.17	9.24	20	-	18.9	12.95	-	2
4 RR5	10.12	24.3	40	100	64	163	63	3
7 RR5	16.51	46.41	70	75	63.2	91	21.3	4
13 RR5	19.58	73.19	130	85.7	18.6	57.7	-32	5
2 RR10	7.03	9.29	40	-	35.45	13.32	-	2
4 RR10	13.03	24.42	80	100	85.35	163.21	63.21	3
7 RR10	21.85	47.13	140	75	67.69	91.64	22.18	4
13 RR10	24.53	74.69	260	85.7	12.26	59.45	-30.6	5
2 RR15	7.73	9.29	60	-	48.94	57.1	-	2
4 RR15	16	24.42	120	100	106.98	162.81	62.9	3
7 RR15	25.78	47.13	210	75	61.12	93	24	4
13 RR15	27.49	74.69	390	85.7	6.7	58.5	-31.7	5
2 RR20	8.2	9.306	80	-	58	13.76	-	2
4 RR20	18.75	24.44	160	100	128.66	162.62	62.62	3
7 RR20	33.52	47.46	280	75	78.77	94.2	25.6	4
13 RR20	37.52	75.45	520	85.7	11.93	58.97	-31.2	5
2 RR25	8.65	9.31	100	-	66.66	13.81	-	2
4 RR25	18.77	24.53	200	100	117	163.48	63.48	3
7 RR25	33.87	47.96	350	75	80.44	95.5	27.33	4
13 RR25	39.45	75.94	650	85.7	46	58.34	-31.9	5

$$\beta = \frac{P_{u_i} - P_{u\,(i-1)}}{P_{u\,(i-1)}} \times 100 \quad (6)$$

$$\alpha = \frac{P_{cr_i} - P_{cr\,(i-1)}}{P_{cr\,(i-1)}} \times 100 \quad (7)$$

$$\gamma = \frac{\beta - Z}{Z} \times 100 \quad (8)$$

Where P_u is ultimate strength pressure (KPa); P_{cr} is the initiation buckling pressure (Kpa).

A comparison is performed with theoretic predictions. Equations on elastic buckling were developed. These equations are indicated in Eq. (9) and Eq. (10)

$$P_{cr} = \gamma . E . \left(\frac{R}{L}\right)^{\alpha} . \left(\frac{t}{R}\right)^{\beta}, \left[(\alpha = 1.02), (\beta = 2.51), (\gamma = 1.033)\right] \quad (9)$$

$$n = 2.47\left(\sqrt{\left(\frac{R}{L}\right)\sqrt{\left(\frac{R}{T}\right)}}\right) \quad (10)$$

Where *n* is theoretic sin wave numbers in Eq. (9) and (10), Young's modulus E has been taken E =211 GPa and R, L, t indicate the radius, space between rings, thickness of specimen shell, respectively. p_{cr}, ^{n} Indicate the elastic buckling of specimen and number of sinus waves on section, respectively.

CONCLUSIONS

The 21 models with diameter to thickness ratios (R/t) equal to 200, have been submitted to damage with magnitudes about 20 and 30% of the respective nominal diameters. The failure mechanism related to the external pressure is governed by cross section instability. The pipe response under external pressure loads shows a sudden lost of strength and All of finite element analysis graphs rise flexibility in buckling and post-buckling region. By increasing the number of rings, initial buckling pressure increases but its propagation speeds up in the post buckling region.

Tangent stress of specimen is the main reason of lateral displacement and Lateral displacement depends on influence of torsion on specimen. Tangent and axial stress have important influence on quality of torsion and geometry of specimen has main influence on number of sinus wave. Comparison of test results with FE models and standards shows a good agreement in both buckling mode and pressure range.

REFFRENCES

1. Golzan, B.S. and H. Showkati, Buckling of thin -walled conical shells under uniform external pressure. J. Thin-walled Struct., 46: 516-529.
2. Jaeyoung lee, P.E., 2008. Introduction to Offshore Pipelines and Risers.
3. Jain, R.K., 2007. Offshore Pipeline Design and Installation, Lecture Notes, Msc Offshore & Ocean Technology, Canfield University, England, February.
4. ABS. 2005. Guide for building and classing subsea pipeline systems and risers. 64–01, American Bureau of Shipping, Houston.
5. Johns, T., R. Mesloh and J. Sorenson, 1976. Propagating buckle arrestors for offshore pipelines. Offshore Technology Conference.
6. Palmer, A.C. and J. Martin, 1975. Buckle propagation in submarine pipelines. Offshore Technology Conference, 1975. *Nature* 254, 46 - 48 (06 March 1975); doi:10.1038/254046a0.
7. Det Norsk Veritas, 2005. DNV – OS – F101 Submarine Pipelines Systems, October 2005.
8. DNV Recommendation Practice, DNV-RP-C201, Buckling Strength of Plated Structures, 2002.
9. Pasqualino, I. and S. Estefen, 2001. A nonlinear analysis of the buckle propagation problem in deepwater pipelines. International J. solids and Structures. 38: 8481-8502.
10. British Standards Institute, PD 8010 Series, 2004. Code of Practice for Pipelines, Part 2: Subsea Pipelines.
11. Toscano, R.G., C. Timms, E.N. Dvorkin and D. DeGeer, 2003. Determination of The Collapse and Collapse Propagation Pressure of Ultra-Deep water Pipelines, Proc. 22nd International Conference on offshore Mechanics and Arctic Engineering, OMAE-37339.
12. Kamalarasa, S. and C. Calladine, 1988. Buckle propagation in submarine pipelines. International J. Mechanical Sci., 30: 217-228.
13. Deng, D. and H. Murakawa, 2006. Numerical simulation of temperature field and residual stress in multi-pass welds in stainless steel pipe and comparison with experimental measurements. Computational materials science. 37: 269-277.
14. Showkati, H. and H. Ansourian, 1995. Influence of Primary Boundary Conditional on The Buckling of Shallow Cylindrical Shells Constructional Steel Research, 36(1): 53-75.
15. Hibbit, Karlsson and Sorensen, Inc. 2009. ABAQUS User's Manual: ABAQUS Standard (I, II, III), Theoretical Manual, ABAQUS Post Manual and Example Problem, Version 6.8.1.
16. Weizbicki, T. and S. Bhat, 2004. On the bifurcation and global energy approach in propagating plasticity, Int. J. Impact Eng., 30: 901-922.
17. Xue, J. and M.S. Hoo Fatt, 2005. Symmetric and anti-symmetric buckle propagation modes in subsea corroded pipelines, Mar. Structure, 18: 43-61.
18. Hoo M.S., Y. Fatt and J. Liu Xue, 2000. Steady-state buckle propagation in corroded pipelines, in: Proceedings of the 10th International Offshore and Polar Engineering Conference, Seattle, 28 May–June 2: 197-204.
19. Kyriakides, S., 2002. Buckle propagation in pipe-in-pipe systems, Part I: experiments, Int. J. Solids Struct, 39(2): 351-366.
20. Kyriakides, S. and T.J. Vogler, 2002. Buckle propagation in pipe-in-pipe systems, Part II: analysis, Int. J. Solids Struct., 39(2): 367-392.